

**EFFECT OF AROMATIC OIL ON PHASE DYNAMICS OF
S-SBR/BR BLENDS FOR PASSENGER CAR TIRE TREADS**

A. Rathi*^a, M. Hernández^b, W.K. Dierkes^a, J.W.M. Noordermeer^a, C. Bergmann^c,
J. Trimbach^c and A. Blume^a

^aUniversity of Twente, Dept. of Elastomer Technology and Engineering, P.O. Box 217, 7500
AE Enschede, The Netherlands

^bDelft University of Technology, Faculty of Aerospace Engineering, Novel Aerospace Materials
Group, Kluyverweg 1, 2629 HS Delft, The Netherlands

^cHansen & Rosenthal KG, Am Sandtorkai 64, 20457 Hamburg, Germany

Presented at the Fall 188th Technical Meeting of the Rubber
Division of the American Chemical Society, Inc.
Cleveland, Ohio
October 14, 2015

ISSN: 1547-1977

ABSTRACT

Even though S-SBR/BR blends are commonly used for passenger car tire treads, little is known about the phase dynamics arising from the local morphological heterogeneities. The present study aims at developing the understanding of: (i) the influence of aromatic oil on the dynamics of the individual phases in S-SBR/BR (50/50) blend, and (ii) the partition of the aromatic oil in either phase.

S-SBR/BR (50/50) blends with varying concentrations of aromatic oil (0/10/20 phr) were studied. Conventional techniques for the determination of T_g (glass transition temperature or α -relaxation process), such as Differential Scanning Calorimetry (DSC) and Dynamic Mechanical Analysis (DMA) were of limited use for fulfilling the goal of the present study. Therefore, Broadband Dielectric Spectroscopy (BDS), a more sensitive technique to study the α -relaxation process was employed. It was possible to de-convolute the dielectric loss (ϵ'') peak of the vulcanized blends into two super-positioned relaxation processes, α' and α (in increasing order of frequency), which were attributed to the S-SBR and BR phases, respectively. The distinct effective T_g 's (T_g^{eff}) of the S-SBR and BR phases varied with the amount of aromatic oil added. T_g^{eff} of the BR phase was close to the T_g of virgin BR, whereas T_g^{eff} of the S-SBR phase was close to the blend average T_g . This is in accordance with the model for phase dynamics of miscible blends by Lodge and McLeish (2000). With this a deeper insight into the dynamic heterogeneity of traditional S-SBR/BR (50/50) blends is obtained.

Key words: S-SBR/BR blends, aromatic oil, phase dynamics, glass transition temperature, dielectric loss (ϵ'')

INTRODUCTION

Tire tread is the outer layer of the tire which makes the contact with the surface of the road. To optimize the overall performance and efficiency of a tire tread, a compounder can play with the type of polymer, amount and type of filler used, amount and type of process aids and the vulcanization system [1]. A good balance of properties can be achieved by using blends of two or three different types of polymers in a tire tread application [2].

Process oil, which acts as a process aid, is an inevitable component in the mixing formulation of a rubber compound for a passenger car tire tread application. It confers numerous advantages to the compound; for example, manufacturing cost reduction, energy saving, reduction of compound viscosities, improving homogeneity of rubber mixes, enabling higher filler loading and hence, better final properties. In a nutshell, the cost to performance ratio of the final compound is improved with the use of process oil [1]. However, little is known about the partitioning of the process oil in the blend compounds, consisting of two or three different types of polymers. This makes it difficult to judge which phase do the compounding ingredients prefer.

A thermorheologically simple polymer system is one in which the molecular mechanisms contributing to time and frequency dependent modulus and compliance functions, have the same temperature dependence [5]. Blends with T_g of components very different from each other are considered thermorheologically complex. The TTS (Time-Temperature Superposition) fails due the thermorheological complexity. For miscible blends such as S-SBR/BR (50/50) blend, where the $T_g(s)$ of the components are very different, thermorheological complexity [3,4,5] can limit the formulation of broadly based mixing rules,

as well as the prediction of blend dynamics and processability. Due to this, it is necessary to apply more sophisticated techniques to study heterogeneity in blend dynamics. Techniques such as NMR spectroscopy [3,4,6-11], neutron spin-echo [12,13], broadband dielectric spectroscopy (BDS) [14-20] can be suitable for this purpose.

The goal of the present research is to study the phase dynamics arising from S-SBR and BR in a 50/50 ratio and two varying concentrations of Treated Distillate Aromatic Extract (TDAE) oil, by means of Broadband Dielectric Spectroscopy (BDS). BDS is known to be a powerful technique to study the dynamics in polymer chains. It allows the investigation of the various motional processes in a polymeric system, which take place on extremely different time scales in a broad frequency and temperature range. It has the ability to cover a broad dynamic range between 10^{-2} to 10^9 Hz in one single run [21]. The main principle of BDS is the sensibility to molecular fluctuations of dipoles within the system. These fluctuations are related to the molecular mobility of groups, segments or whole polymer chains, which can be observed as different relaxation processes [21].

The study of phase dynamics in a blend, arising from S-SBR and BR individually, can provide some interesting hints on the understanding of partitioning of the compounding ingredients in an elastomer compound, especially of the process oil. The consequent quantification of the partitioning of process oil gives an indication to the phase preference of compounding ingredients including the fillers, which are the major determinants of the final in-rubber properties [2].

Conclusive remarks are made on the effect of varying concentrations of TDAE on the segmental dynamics of the individual phases, S-SBR and BR in a 50/50 blend compound. The

extent of the effect of TDAE on each phase is considered to be related to the level of compatibility between the polymers (S-SBR/BR) and oil (TDAE).

EXPERIMENTAL

MATERIALS

The polymers used in this study are widely used by tire manufacturers. The trade name of the S-SBR used is SPRINTAN™ SLR 4602 - Schkopau, manufactured and supplied by Trinseo Deutschland GmbH [22] and the high-cis (>96%) BR is BUNA CB24, supplied by Lanxess Deutschland GmbH [23]. TDAE, the process oil used for this study, is also a very commonly used commercial oil with the trade name, VIVATEC 500, manufactured and supplied by Hansen & Rosenthal KG, Hamburg [24].

The microstructure of the two polymers used in this study, S-SBR and BR, is depicted in Figure 1. The T_g (s) of these raw materials (S-SBR, BR, TDAE), as mentioned in the technical data sheet of the supplier [22-24], are reported in Table I.

MIXING AND COMPOUNDING

The basic compound formulation given on the basis of a total of 100 parts of raw polymer (S-SBR and BR making a total of 100 parts in 50/50 ratio by weight (in phr)) is as follows: S (sulfur) (1.6 phr), ZnO (4 phr), S.A. (stearic acid) (3 phr), CBS (N-cyclohexyl-2-benzothiazole sulphenamide) (2.5 phr), and TDAE (0/10/20 phr). No fillers, antioxidants or other typical processing aids were added to investigate the intended effect more clearly. The compounds were prepared in an internal batch mixer (*Brabender Plasticorder 350S* (390 cc) with *Haake* mixing elements) at 50 °C and 50 rpm. The compounds were mixed in the internal mixer in the first stage. ZnO and stearic acid were added to the polymers after 1.30 (min.secs)

(see Table II). TDAE was added in two steps (by adding 10 phr TDAE) and three steps, (by adding 20 phr TDAE) at the end of the first mixing stage (see Table II). The vulcanization system was added to the compound in a second stage mixing (see Table II), which was carried out on a two roll mill (*Wals Polymix 80T*) at room temperature with friction between the two rolls of 1.25:1. The prepared compounds are referred to as S-SBR/BR (x/y)_0/10/20, where x and y are the respective ratios of the two polymers in the blend, and 0/10/20 are the respective amounts of TDAE in the compounds. The respective components have been referred to as S-SBR/BLEND_0/10/20 or BR/BLEND_0/10/20.

CURING

The samples were vulcanized in a hydraulic press (*Wickert WLP 1600*) at 100 bar and 160 °C into sheets with a thickness of 2 mm, according to their $t_{90} + 2$ minutes optimum vulcanization time, as determined by a Rubber Process Analyzer (*RPA 2000, Alpha Technologies*), following a standard procedure at 160 °C for 45 mins with 1.67 Hz frequency and 13.95% strain.

2 g of green compound are placed in between two steel plates to receive the required thin sheets for the BDS measurements. These (~0.1-0.2 mm) sheets were prepared by vulcanization at t_{90} at 160 °C.

DIFFERENTIAL SCANNING CALORIMETRY (DSC)

Differential scanning calorimeter (DSC) from Netzsch was used to obtain the ‘static’ glass transition temperature of the vulcanized samples. The DSC measurements were carried out using a cooling flow rate of 10 °C/min. A cooling curve was generated by freezing the samples from room temperature (20 °C) up to -150 °C.

DYNAMIC MECHANICAL ANALYSIS (DMA)

Dynamic mechanical analysis of the vulcanized samples was done in the tension mode in a Metravib DMA2000 dynamic spectrometer. The DMA measurements were performed from -150 °C to +80 °C in steps of five degrees at a dynamic strain of 0.5% and frequency of 1 Hz. The glass transition temperatures were obtained from temperature sweep measurements in tension mode.

BROADBAND DIELECTRIC SPECTROSCOPY (BDS)

Dielectric measurements were performed using a high precision dielectric analyzer (ALPHA analyzer, Novocontrol Technologies). The vulcanized, thin sheets of rubber were cut in a disk shape and were mounted in the dielectric cell between two parallel gold plated electrodes. The complex dielectric permittivity, ϵ^* ($\epsilon^* = \epsilon' - i\epsilon''$) was measured by performing consecutive isothermal frequency sweeps (10^{-1} - 10^7 Hz) in the temperature range from -120 °C to +80 °C in steps of 5 °C.

RESULTS AND DISCUSSIONS

The mechanically blended and vulcanized series of S-SBR/BR (50/50) blends with varying concentrations of TDAE, 0/10/20 phr, have been characterized using DSC, DMA and BDS. A combination of the traditional techniques (DSC, DMA) and the more sophisticated relaxation spectroscopic (BDS) techniques has been utilized to study the component phase dynamics in the blends studied. A deconvolution of the ‘apparently’ coupled relaxation dynamics of S-SBR and BR phases in a series of TDAE-extended S-SBR/BR (50/50) blends is discussed in this section. Glass transition temperature (α -relaxation process) is the main property on which this study is based because it is known to be the most important property which can give an indication up to a large extent on the three main performance indicators for a

tire tread, rolling resistance (RR), abrasion resistance (AR) and wet skid resistance (WSR) [25-28].

Literature on S-SBR/BR blends has suggested that these blends are conditionally compatible [2,29]. It has been reported for the S-SBR blends that a high vinyl SBR is miscible with low vinyl BR due to the repulsion between the vinyl and styrene units on the same SBR chain. Therefore, the S-SBR with high vinyl (ca. 50%) content and the BR with high cis (> 96%) and low vinyl (<1%) content were chosen for this study. Therefore, it was expected that a blend of these two polymers is thermodynamically miscible [29].

In all vulcanized blends, a single DSC transition as well as a single $\tan \delta$ peak from dynamic mechanical studies was obtained (see Figure 2 and 3). These results give a first confirmation for the miscibility of the S-SBR/BR (50/50) blends studied. But the presence of the single peaks from DSC and DMA measurements limits further study pertaining to the phase preference by the TDAE oil.

Hence, BDS investigations were performed for the S-SBR/BR (50/50) compounds with varying concentrations of TDAE. Figure 4 shows a representative 3D dielectric dispersion curve [31-32], as obtained from BDS for the S-SBR/BR (50/50) blend without TDAE, where the presence of a single broad and asymmetric relaxation can be noted in the temperature range, which can be associated to the glass transition. This broad dielectric loss peak is assigned to the collective contribution of both the polymers in the 50/50 blend, S-SBR and BR. Although not shown in this paper but known from further studies, other oil-extended blends present a similar dielectric behavior. For all blends studied, the single, broad relaxation which is observed on the 3D plot lies in between the two contributing relaxations of S-SBR and BR. There is a shift in this peak depending on the amount of the TDAE in the investigated

compounds. The shift in the α -relaxation peak based on the different blend ratios is elaborated upon in the further discussion.

The Havriliak-Negami equation can be used to deconvolute a collective dielectric loss spectra into its contributions. Therefore, the study was focused on the deconvolution of the broad dielectric loss peak into its two contributing phases, S-SBR and BR, expected in increasing order of frequency.

Figure 5 describes the shift in the peak of the normalized dielectric spectra (ϵ'' versus frequency) for the pure polymers, S-SBR, BR, and TDAE-extended S-SBR/BR blends in varied phr(s), 0/10/20. These curves were normalized to the ϵ''_{\max} for the ease of comparing them at different temperatures. It can be clearly seen in all these spectras that the peak of the dielectric loss moves to higher frequencies as the temperature increases. This shift in the frequency of the maximum loss gives evidence for this relaxation process to be a thermally activated process [30].

It is evident that the shape of the dielectric dispersion curves for the blends is not typical, they are broad and asymmetric, unlike a typical dielectric dispersion [33,34] plotted in the frequency domain. When compared to the similar curves for S-SBR and BR, it is noted that the loss spectras for the blends are lying in between that of the two components, depending on the blend ratio. The peak of the loss spectra shifts in the direction of the component in higher majority in the blend. This is the first hint to the presence of more than one relaxations producing a collective relaxation due to the presence of binding crosslinks and the thermodynamic compatibility between the two types of polymer chains, S-SBR and BR.

The asymmetric dielectric relaxation spectras were further investigated by attempting to fit them using the Havriliak-Negami (HN) equation, which describes a dielectric relaxation

process in terms of a characteristic relaxation time (τ_{HN}) at the frequency of maximum loss. The dielectric spectrum for each of the blends was analyzed and the experimental data of ε'' versus frequency was fitted with the representative Havriliak-Negami (HN) equation [21,34-36] which is stated as follows,

$$\varepsilon_{\text{HN}}^*(\omega) = \varepsilon_{\infty} + \frac{\Delta\varepsilon}{[1 + (i\omega\tau_{\text{HN}})^b]^c} \quad (1)$$

where, τ_{HN} is the characteristic Havriliak-Negami relaxation time, which represents the most probable relaxation time from the relaxation time distribution function, $\Delta\varepsilon$ (relaxation strength) = $\varepsilon_s - \varepsilon_{\infty}$, ε_{∞} and ε_s are the unrelaxed and relaxed values of the dielectric constant, ω is the frequency, $\varepsilon_{\text{HN}}^*(\omega)$ is the frequency dependent Havriliak-Negami complex dielectric permittivity, and b and c are the shape parameters, which describe the symmetric and asymmetric broadening of the relaxation time distribution function, respectively.

τ_{HN} is related to the frequency of maximum loss [21,34,37], $F_{\text{max}} = 1/2\pi\tau_{\text{max}}$ by the following equation:

$$\tau_{\text{max}} = \frac{1}{2\pi F_{\text{max}}} = \tau_{\text{HN}} \left[\sin \frac{b\pi}{2+2c} \right]^{-1/b} \left[\sin \frac{bc\pi}{2+2c} \right]^{1/b} \quad (2)$$

Where, F_{max} is the frequency of maximum loss, which is related by the above equation to τ_{max} , the relaxation time of maximum loss.

Interestingly, it was not possible to achieve a proper fit for the blend samples in this study by using a single HN equation. Therefore, two HN equations were used plus a conductivity contribution to achieve a satisfactory fit of the measurement data. The success of

the fittings done using two HN equations proves the presence of two superpositioned HN relaxation processes, referred to as α and α' , in increasing order of frequency. The α and α' (in increasing order of frequency) can be assigned as the S-SBR and BR phases of the blends due to the greater mobility of BR compared to S-SBR. The steric hindrances in S-SBR chains due to the presence of the styrene group in the main chain causes a slowdown in the dynamics of S-SBR chains.

The relaxation parameters ($\Delta\varepsilon_{\alpha'}$, $\Delta\varepsilon_{\alpha}$, b , b' , c , c' , $\tau_{HN}(\alpha)$ and $\tau_{HN}(\alpha')$) describing each successful fit of experimental data are calculated with each fitting. The nature of HN fittings is 'flexible' [33] which makes it difficult to obtain a fit that satisfies the experimental data as well as gives physically meaningful values. To overcome this, an own protocol was devised to perform these fittings wherein changes in the b and c parameters for the α phase were allowed and the c' parameter to 1 for the α' phase was fixed [34]. This was done to force a symmetric shape and thus maintain a narrow distribution of relaxation times. Without such an approach, it is extremely difficult to fit an asymmetric broad peak with two physically meaningful contributions.

The representative fittings with the deconvoluted, superpositioned relaxation processes assigned as S-SBR and BR, in increasing order of frequency at an appropriate temperature ($T = -30$ °C) are shown in Figure 6. In all the curves in Figure 6, the collective relaxation spectrum is shown, which was fitted and deconvoluted into two superpositioned process that are depicted as dashed lines, α phase, BR and α' phase, S-SBR. There is also a conductivity contribution (shown as dotted line) which is used to achieve a better fit of the tailing ends of the spectra. The representative values of the fittings for the three blend samples at their respective temperatures of well-resolved deconvolutions are presented in Table III.

A shift in the loss spectra and the individual components, S-SBR and BR is observed as the amount of oil is varied in the blend compounds (Figure 6). This provides an opportunity to quantify the effect of TDAE on the two components in the blend studied. A greater shift in the BR component can be recognized as compared to S-SBR. The greater shift in BR is even more clear on the activation plot (Figure 7), which will be elaborated upon in the further discussion.

As described earlier, the relaxation times for both the α and α' phase were obtained from a HN curve fit to the peak maximum frequency at each temperature. The $\tau_{\text{HN}}(\alpha)$ and $\tau_{\text{HN}}(\alpha')$ for the deconvoluted phases in each blend, can be converted to the respective τ_{max} using equation 2. Figure 7 shows some relaxation times plotted as a function of the inverse temperature.

The temperature dependence of τ_{max} is governed by the Vogel-Fülcher-Tamman (VFT) equation [21,30,35] which is stated as follows,

$$\tau_{\text{max}} = \tau_0 \exp\left(\frac{B}{T - T_0}\right) \quad (3)$$

Where, τ_{max} is the relaxation time at the frequency of maximum loss, τ_0 and B are empirical parameters, and T_0 is the ideal glass transition or Vogel temperature, which is generally 30-70 K below T_g . For avoiding the effect of misleading parameters, a value of $\log \tau_0 = 14$ is adapted for the data fitting using the VFT equation, based on the study of Angell [38].

Since the temperature dependence of the τ_{max} from the S-SBR and BR phases follows the VFT behavior (see Figure 7), this proves the presence of two polymeric phases in the blends. The effective T_g (T_g^{eff}) of the two phases in each blend can now be estimated as the temperature at $\tau_{\text{max}} = 100$ seconds, which is the convention for estimating the T_g by BDS [39].

The clear segregation in the segmental dynamics can be seen from the Figure 7. The two effective phases arising from S-SBR and BR, in a non-oil-extended 50/50 blend, are placed significantly apart from each other on the activation plot (see Figure 7). Moreover, they seem to converge at higher temperatures, which is a characteristic feature of segmental dynamics as well as VFT curves. It is assumed that the segmental dynamics arising from all systems equalize at very high temperatures, hence, VFT curves for segmental dynamics seem to converge at higher temperatures [21]. The same behavior is true for oil-extended blends studied. Also, a clear shift in the T_g^{eff} for the respective phases S-SBR and BR for the oil-extended blends is observed. The degree of shift is greater for the BR phase as compared to the S-SBR phase. This goes hand in hand with the degree of shift in the oil-extended pure polymers (see Figure 7 A)). A greater shift occurs in the segmental dynamics of oil-extended BR [1]. An interesting observation here is that the direction of the shift in case of the oil-extended pure polymers was opposite to each other. For instance, the shift for oil-extended BR was towards the left on the activation plot, which indicates a restricting effect on the segmental dynamics of the BR chains. However, for S-SBR, the shift was towards the right on the activation plot, which indicates a plasticizing effect on the S-SBR chains. Ideally, the same direction of shift would be expected for the effective phases arising from S-SBR and BR in a 50/50 blend. But a restricting effect was observed i.e., in both the effective phases, S-SBR and BR, in a series of oil-extended blends with 0/10/20 phr of TDAE (see Figure 7B)). The restricting effect seen in the effective S-SBR phase can be ascribed to the effect of interferences from the BR chains on the segmental dynamics of S-SBR. Likewise is applicable to the reduced degree of shift in the BR phase.

The T_g^{eff} of each component obtained by BDS are compared to the T_g^{eff} predicted through the theoretical models available for predicting the dielectric response of phases in miscible blends. There are a few models available to predict the dielectric response in miscible blends. The details about these models can be found elsewhere [3-4,40-41]. The model used as a part of this study is the model for phase dynamics of miscible blends by Lodge and McLeish [41].

The Lodge and McLeish model is based on predicting the T_g^{eff} that the two components experience within a miscible blend. It postulates that in a miscible blend, the local environment of a monomer of type A will, on average, be richer in A compared to the bulk composition, ϕ . A similar effect is expected for B. This is a direct consequence of chain connectivity. By assigning a length scale or volume to a component dynamic mode, the relevant ‘self-concentration’, ϕ_s can be estimated. In this model, the Kuhn length (l_K) is the chosen length scale.

$$\phi_s = \frac{C_\infty M_0}{k \rho N_{av} V} \quad (4)$$

where C_∞ is the characteristic ratio, M_0 is the repeat unit molar mass, k is the number of backbone bonds per repeat unit, V is the volume occupied by a segment of the length scale same as l_K ($V \sim l_K^3$), ρ is the density and N_{av} is the Avogadro’s number [42].

An effective local composition ϕ_{eff} was calculated from ϕ_s and ϕ .

$$\phi_{\text{eff}} = \phi_s + (1 - \phi_s) \phi \quad (5)$$

The T_g^{eff} for each phase was then calculated using a modified Fox equation.

$$\frac{1}{T_g^{\text{eff(BR)}}(\phi_{\text{eff(BR)}})} = \frac{\phi_{\text{eff(BR)}}}{T_{g,S-SBR}} + \frac{1 - \phi_{\text{eff(BR)}}}{T_{g,BR}} \quad (6)$$

Where $T_g^{\text{eff(BR)}}$ is the effective T_g of the BR phase, $\phi_{\text{eff(BR)}}$ is the effective concentration of the BR phase, $T_{g,S-SBR}$ is the T_g of S-SBR and $T_{g,BR}$ is the T_g of BR. Similar equation is valid for the S-SBR phase for its effective T_g calculation in a blend.

As stated in the model, the T_g^{eff} of the component with lower T_g is closer to that of the pure polymer due to its flexible nature which leads to a larger ϕ associated with it. The higher T_g component is expected to have lower ϕ associated with it thus, its dynamics and T_g^{eff} in a mixture would be more representative of the blend composition. The results obtained from BDS are in close correlation with the T_g^{eff} as calculated from the model. A deviation from the values expected by the model for the S-SBR phase in a 50/50 blend can be seen in Table IV. This can be reasoned in two ways, i) the calculations are based on available data for typical SBR and BR polymers whereas, the polymers used are the new grade commercial polymers, ii) there is a slight masking of the S-SBR phase dynamics in the blends which is supported by a lower contribution of the S-SBR phase in Figure 6. It is possible that the BR phase, which has a more flexible nature and faster relaxation dynamics can overshadow the contribution of the S-SBR phase with slower relaxation dynamics and, as a consequence of this, shows an T_g^{eff} closer to the T_g of the BR phase. Apart from this one phase, these results are well corroborated with the theoretical model by Lodge and McLeish. Therefore, it reassures the credibility of the fitting protocol used and the deconvolution of the two phases in miscible S-SBR/BR (50/50) blends.

The T_g values from this model of the studied blend compounds and the experimentally obtained phase $T_g(s)$ are presented in Table IV. The model presented closely corroborating

values with the 50/50 blend without oil but for the oil-extended compounds, it was not coherent with experimentally obtained data. This is a reasonable observation due to the fact that the Lodge and McLeish model is applicable to the prediction of T_g^{eff} of the two phases in a blend, not for the effect of compounding ingredients in the blends.

Through this work a new way for the prediction of the viscoelastic response was presented for miscible blend [41] solely on the basis of the composition and the component architectures.

CONCLUSIONS

The following are the conclusions which can be drawn from the study presented in this manuscript:

- i. S-SBR/BR (50/50) blends studied are miscible blends, which is confirmed by the presence of a single transition signal observed from DSC, DMA and BDS.
- ii. The phase dynamics of the S-SBR and BR phases in the S-SBR/BR (50/50) blend can be decoupled, through the use of a fitting protocol based on the Havriliak-Negami equation, from the ‘apparently’ coupled relaxation dynamics, as observed from BDS investigations.
- iii. The effect of TDAE (process oil) on the individual phases in a S-SBR/BR (50/50) blend is clearly seen. It is evident that the greater effect of the TDAE is observable for the BR phase.
- iv. T_g^{eff} of the two phases in the blend compounds studied are calculated from the activation plot. The values of T_g^{eff} from BDS for the 50/50 blend without oil, are corroborated

with the Lodge and McLeish model for dynamics of miscible blends. The model available is applicable only to the non-oil-extended blends.

v. This work presents an alternative to overcome the thermorheological complexities in miscible blends with a very high difference in the $T_g(s)$ of both the components.

FUTURE OUTLOOK

The ultimate goal from this research is to achieve a quantification of the partitioning of TDAE oil in each phase of the S-SBR/BR (50/50) blend. The aim is also to extend the protocol devised for the 50/50 blend to other blend ratios, such as 70/30 and 30/70, to study the effect of blend ratio on the partitioning of TDAE.

ACKNOWLEDGEMENTS

The authors are indebted to H&R Ölwerke Schindler GmbH (Hamburg, Germany) for their scientific, financial and materials support of the current project as well as the permission to publish this work.

REFERENCES

- [1] A. Rathi, M. Hernández, C. Bergmann, J. Trimbach, W.K. Dierkes, A. Blume, *Kautschuk. Gummi. Kunstst.*, Submitted (2015).
- [2] T.R. Maier, *PhD Thesis*, Case Western Reserve University, Ohio, The United States (1995).
- [3] S. Shenogin, R. Kant, R.H. Colby, S.K. Kumar, *Macromolecules*, 40, 5767 (2007).
- [4] Y. Hirose, O. Urakawa, K. Adachi, *Macromolecules*, 36, 3699 (2003).

- [5] J.E. Mark, *Physical Properties of Polymers Handbook*, p 450, 455 (2007).
- [6] S.A. Madbouly, *Polymer Journal*, 34, 515 (2002).
- [7] J. Colmenero, A. Arbe, *Soft Matter*, 3, 1474 (2007).
- [8] W.G.F. Sengers, M. Wübbenhorst, S.J. Picken, A.D. Gotsis, *Polymer*, 46, 6391 (2005).
- [9] D. Boese, F. Kremer, *Macromolecules*, 23, 829 (1990).
- [10] B.B. Sauer, P. Avakian, G.M. Cohen, *Polymer*, 33, 2666 (1992).
- [11] S. Cervený, R. Bergman, G.A. Schwartz, P. Jacobsson, *Macromolecules*, 35, 4337 (2002).
- [12] D. Richter, R. Zorn, B. Farago, B. Frick, L. J. Fetters, *Phys. Lett.*, 68, 71 (1992).
- [13] D. Richter, M. Monkenbusch, A. Arbe, J. Colmenero, B. Farago, *Physica B*, 1005, 241 (1998).
- [14] V.M. Litvinov, *Macromolecules*, 39, 8727 (2006).
- [15] K. Saalwächter, A. Heuer, *Macromolecules*, 39, 3291 (2006).
- [16] Y. He, T.R. Lutz, M.D. Ediger, *Macromolecules*, 37, 9889 (2004).
- [17] H. Luo, M. Klüppel, H. Schneider, *Macromolecules*, 37, 8000 (2004).
- [18] K. Saalwächter, M. Klüppel, H. Luo, H. Schneider, *Appl. Magn. Reson.*, 27, 401 (2004).
- [19] G.C. Chung, J. A. Kornfield, S.D. Smith, *Macromolecules*, 27, 964 (1994).
- [20] J. O'Brien, E. Cashell, G.E. Wardell, V.J. McBrierty, *Macromolecules*, 9, 653 (1976).
- [21] M. Hernández, *PhD Thesis*, Universidad Complutense de Madrid, Spain (2012).
- [22] Technical Data Sheet- SPRINTAN™ SLR 4602 – Schkopau, Trinseo Deutschland GmbH.

- [23] Technical Data Sheet- BUNA CB24, Lanxess Deutschland GmbH.
- [24] Technical Data Sheet- VIVATEC 500, H&R Ölwerke Schindler GmbH, Hamburg.
- [25] K.H. Nordsiek, *Kautschuk. Gummi. Kunstst.*, 25, 87 (1972).
- [26] K.H. Nordsiek, *Kautschuk. Gummi. Kunstst.*, 39, 599 (1986).
- [27] K.H. Nordsiek, ACS Rubber Division Meeting, Indianapolis, U.S.A. (1984).
- [28] W.A. Schneider, F. Huybrechts, K.H. Nordsiek, *Kautsch. Gummi Kunstst.*, 44, 528 (1991).
- [29] S. Sakurai, T. Izumitani, H. Hasegawa, T. Hasimoto, C.C. Han, *Macromolecules*, 24, 4844 (1991).
- [30] M. Hernández, J. Carretero-González, R. Verdejo, T.A. Ezquerra, M.A. López-Manchado, *Macromolecules*, 43, 643 (2010).
- [31] R.A. Kalgaonkar, J.P. Jog, *J. Polym. Sci.:Part B: Polym. Phys.*, 46, 2539 (2008).
- [32] R. Kunanuruksapong, A. Sirvat, *Appl. Phys. A*, 92, 313 (2008).
- [33] R. Zorn, F.I. Mopsik, G.B. McKenna, L. Willner, D. Richter, *J. Chem. Phys.*, 107 3645 (1997).
- [34] M. Hernández, T.A. Ezquerra, R. Verdejo, M.A. López-Manchado, *Macromolecules*, 45, 1070 (2012).
- [35] J.P. Runt and J.J. Fitzgerald, *Dielectric Spectroscopy of Polymeric Materials*, p 81, 227,262 (1997).
- [36] Havriliak, S.; Negami, S. *Polymer*, 8, 161 (1967).
- [37] Richter, R.; Angell, C.A. *J. Chem. Phys.*, 108 , 9016 (1998).

[38] C.A. Angell, *Polymer*, 38, 6261 (1997).

[39] C.A. Angell, *J. Non-Crystalline Solids*, 131, 13 (1991).

[40] Y. He, T.R. Lutz, M.D. Ediger, *Macromolecules*, 37, 9889 (2004).

[41] T. P. Lodge, T. C. B. McLeish, *Macromolecules*, 33, 5278 (2000).

Table I

T_g (s) of the raw materials (S-SBR, BR, TDAE), as mentioned in the technical data sheet of the supplier [22-24]

Material	T_g (s)
S-SBR	-25 °C
BR	-109 °C
TDAE	-49 °C

Table II

MIXING PROTOCOL

1st Stage: Internal Mixer	1st Stage: Internal Mixer	1st Stage: Internal Mixer
Sample: No oil	Sample: 10 phr TDAE	Sample: 20 phr TDAE
Rotor speed: 50 RPM	Rotor speed: 50 RPM	Rotor speed: 50 RPM
Initial temp. setting: 50 °C	Initial temp. setting: 50 °C	Initial temp. setting: 50 °C
Fill factor: 0.7	Fill factor: 0.7	Fill factor: 0.7
Actions	Actions	Actions
(Min. sec.)	(Min. sec.)	(Min. sec.)
0.30 Add Polymers	0.30 Add Polymers	0.30 Add Polymers
1.30 Add ZnO and Stearic acid	1.30 Add ZnO and Stearic acid.	1.30 Add ZnO and Stearic acid
4.00 Dump	2.40 Add 15 ml TDAE	2.40 Add 15 ml TDAE
	5.00 Add 9 ml TDAE	5.00 Add 15 ml TDAE
	7.00 Dump	8.00 Add 14 ml TDAE
		10.30 Dump

2nd Stage: Two roll mill
Sample: All samples
Friction ratio: 1.25:1
Room Temperature
Actions
(Min. sec.)
0.0 Add batch from stage 1.
0.30 Add curatives
5.00 Dump

TABLE III

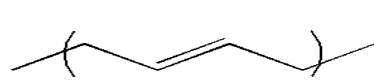
HN fitting parameters for the deconvoluted relaxation spectra of S-SBR/BR (50/50) blends with varying concentrations of TDAE at T=-30 °C.

S-SBR/BR (50/50)	$\Delta\varepsilon_a$	$\Delta\varepsilon_{a'}$	$\tau_{HN}(a)$ (s)	$\tau_{HN}(a')$ (s)	b	b'	c	c'
No oil	0.226	0.089	1.384×10^{-4}	5.317×10^{-4}	0.609	0.429	0.131	1
10 phr TDAE	0.678	0.281	1.509×10^{-4}	6.502×10^{-4}	0.692	0.460	0.112	1
20 phr TDAE	0.254	0.130	2.000×10^{-4}	1.100×10^{-3}	0.584	0.445	0.231	1

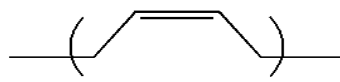
TABLE IV

Comparison of the T_g^{eff} of the S-SBR and BR phases as calculated by the Lodge and McLeish Model and the experimentally obtained values from BDS.

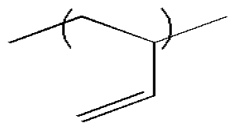
S-SBR/BR (50/50)	Phase	T_g^{eff} (Model based)	T_g^{eff} (BDS)
No oil (0 phr TDAE)	S-SBR	-42.10 °C	-43.07 °C
	BR	-59.65 °C	-69.45 °C
10 phr TDAE	S-SBR	-	-38.32 °C
	BR	-	-58.44 °C
20 phr TDAE	S-SBR	-	-36.50 °C
	BR	-	-54.16 °C



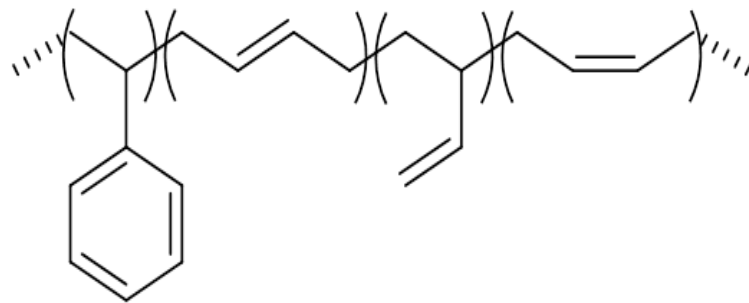
1,4-trans-polybutadiene



1,4-cis-polybutadiene



1,2-polybutadiene

Polybutadiene (BR)**Solution-Styrene
Butadiene Rubber (S-SBR)****Figure 1. Microstructure of BR^a and S-SBR^b**^aR.H. Grubbs, C.W. Bielawski, US6410666B1 (2002)^bTechnical data by the supplier

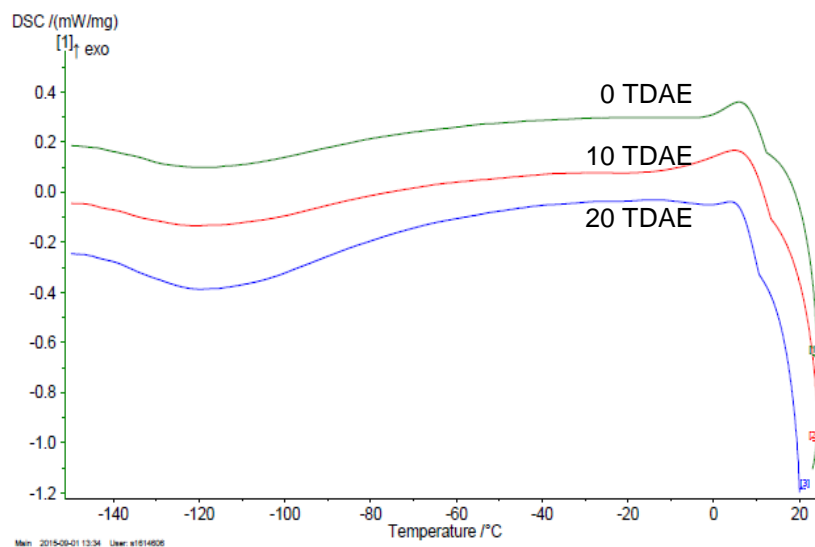


Figure 2. DSC curve for the S-SBR/BR blends in 50/50 ratio with, A) No oil (0 phr TDAE), B) 10 phr TDAE, and C) 20 phr TDAE.

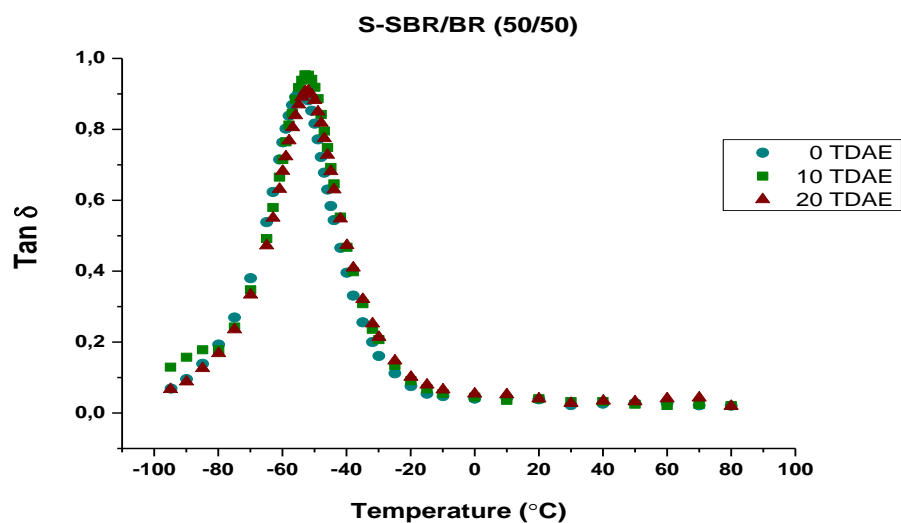


Figure 3. Tan δ vs. Temperature curve for S-SBR/BR blends in 50/50 ratio with, A) No oil (0 phr TDAE), B) 10 phr TDAE, and C) 20 phr TDAE.

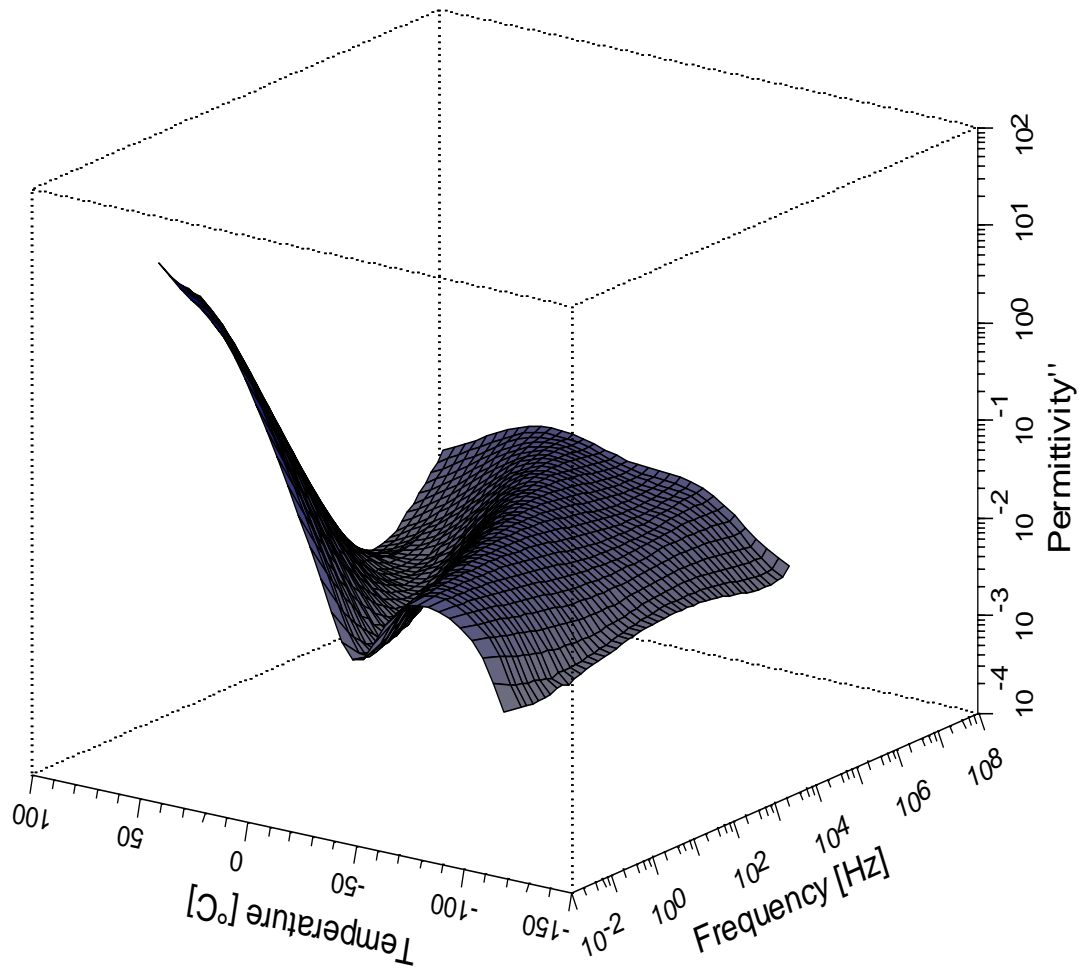


Figure 4. 3D curve of S-SBR/BR (50/50) blend as obtained from BDS.

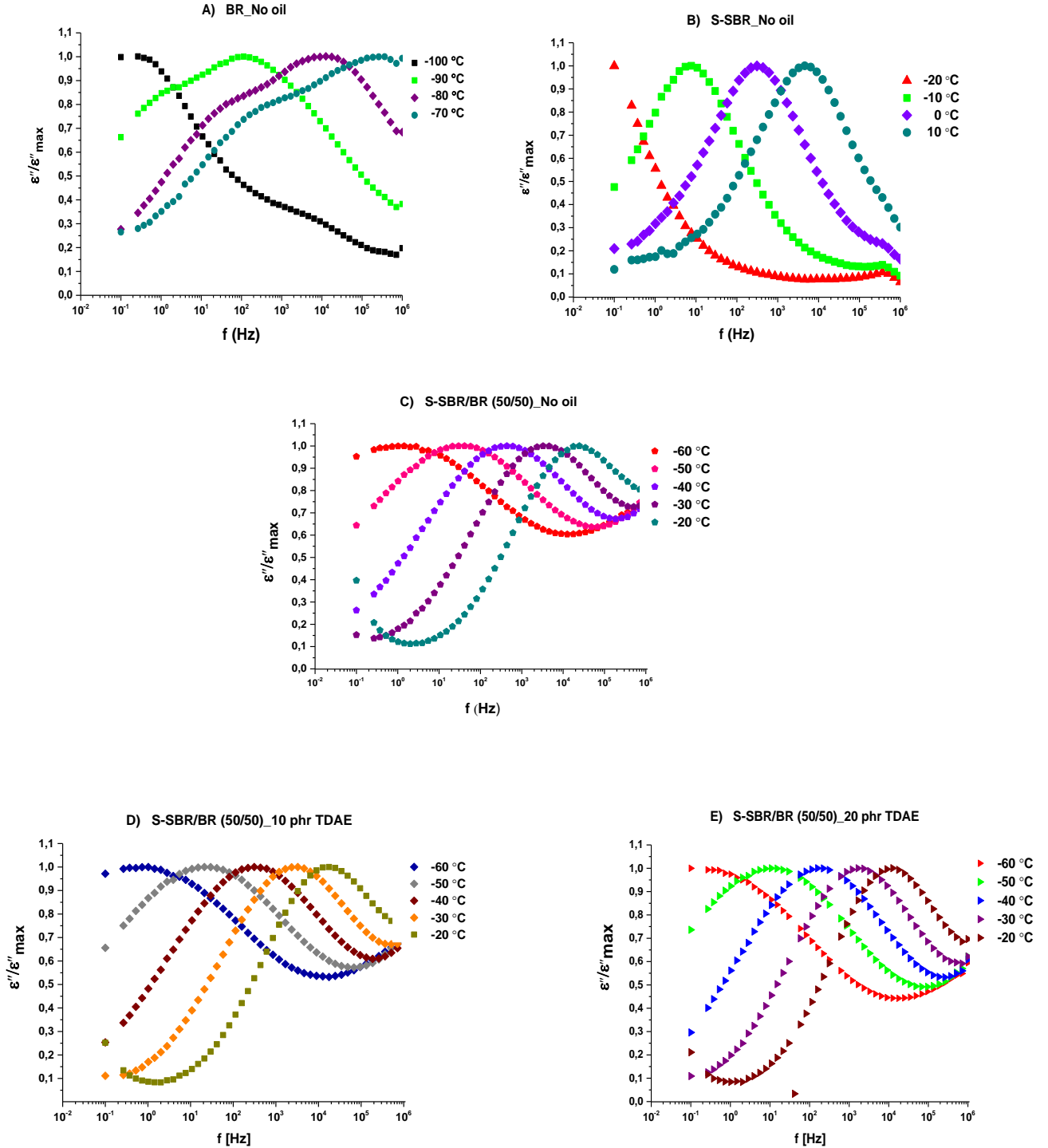


Figure 5. Normalized ε'' versus frequency in the region of segmental mode for A) BR without TDAE, B) S-SBR without TDAE, and S-SBR/BR blends in 50/50 ratio with, C) No oil, D) 10 phr TDAE, and E) 20 phr TDAE.

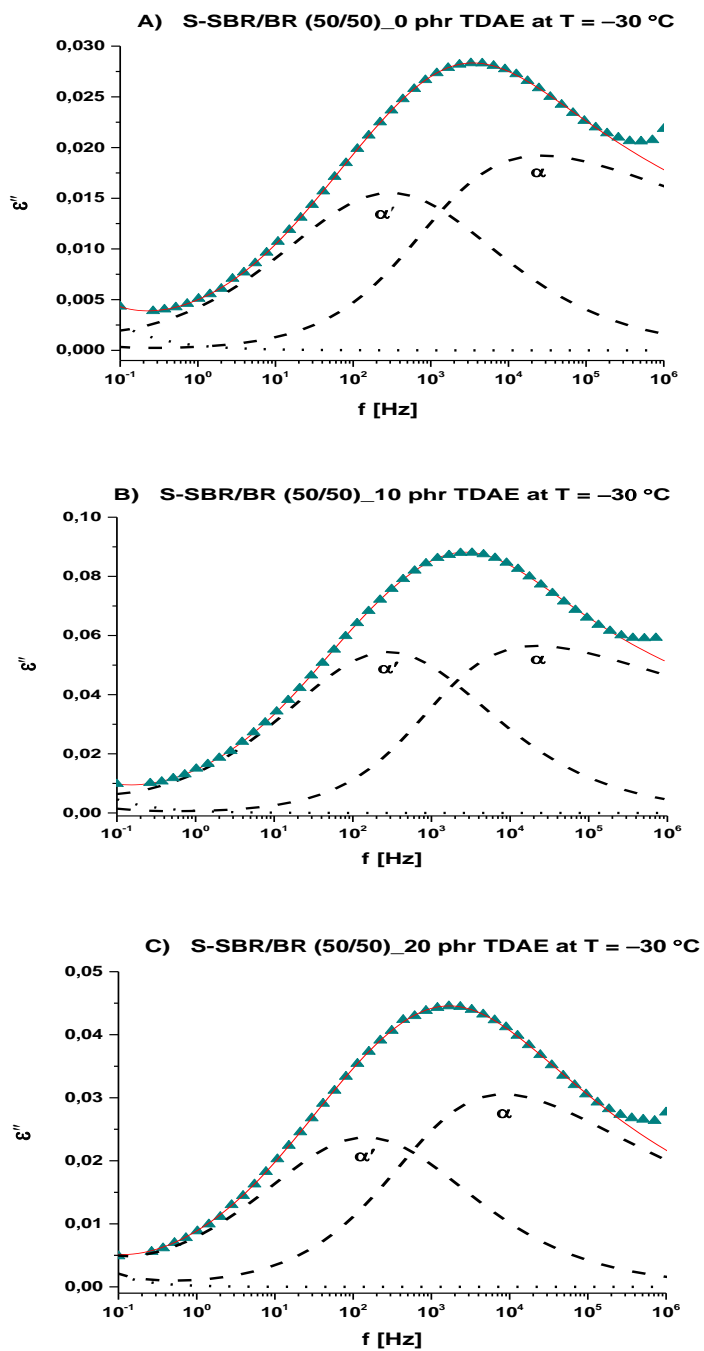


Figure 6. Deconvolution results from fitting of the α' and α phases using 2 Havriliak-Negami (HN) equations for the S-SBR/BR blends in 50/50 ratio with, A) No oil, B) 10 phr TDAE, And C) 20 phr TDAE.

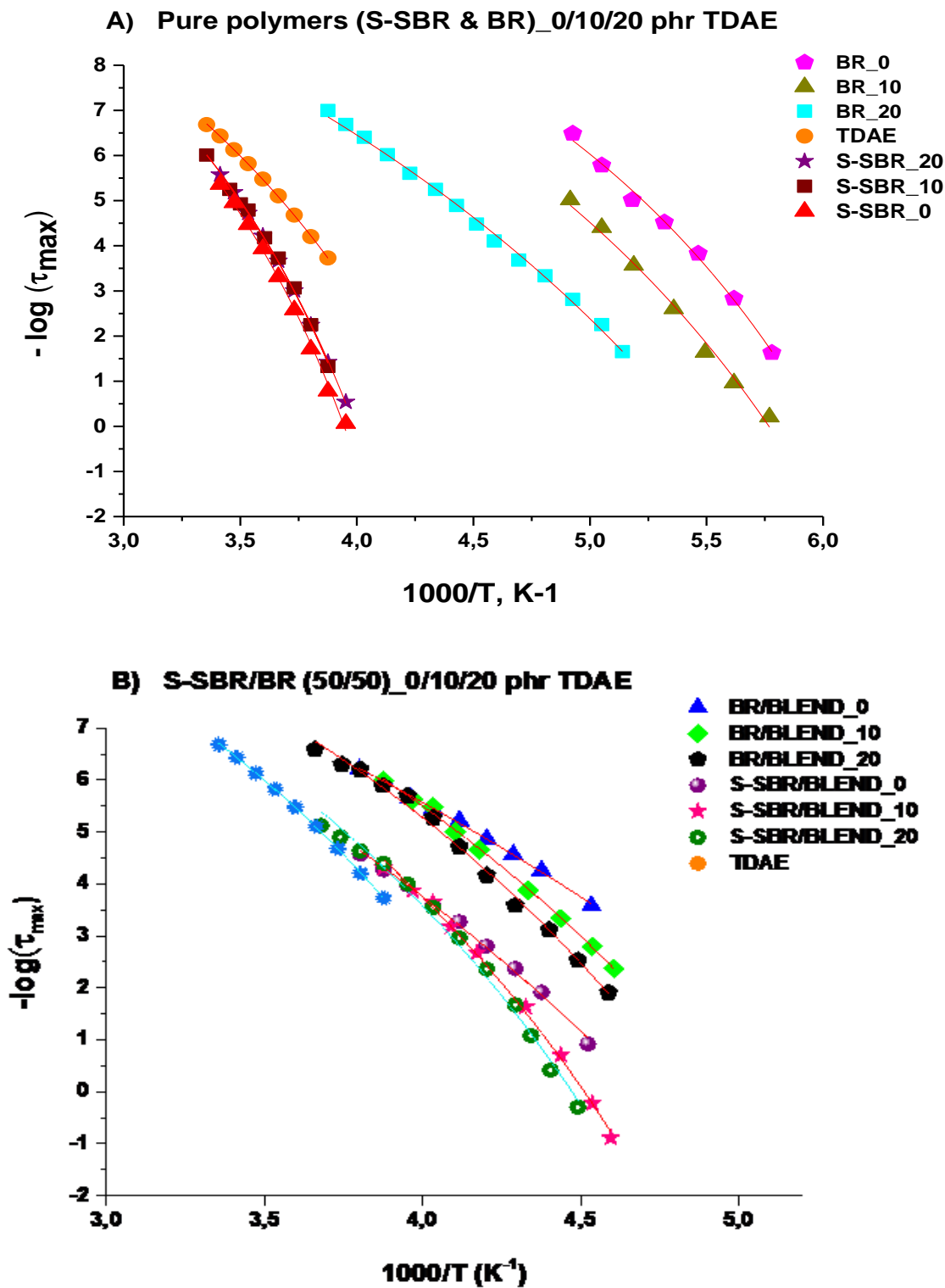


Figure 7. Activation plot showing the shift in the temperature dependence of the average relaxation times of the, A) Pure polymers (S-SBR and BR) and B) S-SBR and BR phases in the S-SBR/BR (50/50) blends, with varied amounts of TDAE oil.

List of figures:

Figure 1: Microstructure of BR^a and S-SBR^b

Figure 2: DSC curve for the S-SBR/BR blends in 50/50 ratio with, A) No oil (0 phr TDAE), B) 10 phr TDAE, and C) 20 phr TDAE.

Figure 3: Tan δ vs. Temperature curve for S-SBR/BR blends in 50/50 ratio with, A) No oil (0 phr TDAE), B) 10 phr TDAE, and C) 20 phr TDAE.

Figure 4: 3D curve of S-SBR/BR (50/50) blend as obtained from BDS.

Figure 5: Normalized ε'' versus frequency in the region of segmental mode for A) BR without TDAE, B) S-SBR without TDAE, and S-SBR/BR blends in 50/50 ratio with, C) No oil, D) 10 phr TDAE, and E) 20 phr TDAE.

Figure 6: Deconvolution results from fitting of the α' and α phases using 2 Havriliak-Negami (HN) equations for the S-SBR/BR blends in 50/50 ratio with, A) No oil, B) 10 phr TDAE, And C) 20 phr TDAE.

Figure 7: Activation plot showing the shift in the temperature dependence of the average relaxation times of the, A) Pure polymers (S-SBR and BR) and B) S-SBR and BR phases in the S-SBR/BR (50/50) blends, with varied amounts of TDAE oil.